



Original Research Article

A study of artificial intelligence - Based machine learning and radiomic texture features in Parkinson's (Outcome of subthalamic nucleus deep brain stimulations analysis)

Venkateshwarla Rama Raju^{1-3*}

¹CMR College of Engineering & Technology, Affili: Jawaharlal Nehru Technological University JNTU, Hyderabad, Telangana, India

²CMR Institute of Medical Sciences, and CMR Hospital, Kandlakoya, Hyderabad, Telangana, India

³Nizam's Institute of Medical Sciences, NIMS Hospital, Hyderabad, Telangana, India

Abstract

Background: Goal of this study is to apply AI-based machine learning and advanced radiomic textures in Parkinson's, to predict subthalamic-nucleus(STN) outcome of Parkinson disease patients' stimulations done with deep brain stimulators by applying the radiomic techniques such that quantifiable image/signal-features' or textures extrapolated.

Materials and Methods: Parkinson subjects (Parkinson diseased patients) were recruited in this study. Subjects with advanced PD of >5 years with good response to L-Dopa and H and Y score of <4 with normal cognition were eligible for electrode implantations. Implantation was planned by applying a CRW frame with an MRI protocol using a sophisticated AI-Frame link computer/software with 5 channels and intra op microelectrode- recording (MER). MER was performed in all subjects extending ± 10 mm (above/below STN neurons targets). Ultimate target choice was based on dyskinesias of induced macro stimulus plus proven by post op MRI. Subjects 5 underwent DBS implantation at STN site. 5 subjects (34~5%) showed mean DBS motor outcome. 9 amygdalē-nuclei, 12 hippocampus subfields were segmented with Free surfer 7.0 version pipeline from pre op MRI. An "Py-Radiomics" platform running under free surfer operating system-software was employed to extrapolate 120 textures ('radiomic-features') for every nucleus and sub field ensuing in 5,040 feature-manifestations. The m.R.M.R feature-selection technique was employed to reduce the number-of-features to 20, 8 AI-based ML techniques: normalized-binary logistic regression (LR), decision tree classifier (DT), naïve yes classifier (NB), kernel support vector machines(SVMs), feed-forward neuronal network-based auto encoder for anomaly detection(DNN-A) were applied to build the models for poor-versus-good and very good STN-DBS motor outcome prediction.

Results: The highest mean prediction accuracy was obtained using normalized linear-regression ($96.65 \pm 7.24\%$, AUC: 0.98 ± 0.06) and DNN ($87.25 \pm 14.80\%$, AUC: 0.87 ± 0.18).

Conclusion: Findings reveal the potential power of radiomic-features achieved from hippocampus and amygdalē MRI within the prediction of STN-DBS motor outcomes for PD subjects.

Keywords: Amygdalē, Deep brain stimulation, Hippocampus, Motor outcome, Parkinson disease, Prediction, Radiomic features, Radiomics, Textures.

Received: 21-05-2025; **Accepted:** 03-07-2025; **Available Online:** 15-07-2025

This is an Open Access (OA) journal, and articles are distributed under the terms of the [Creative Commons Attribution-NonCommercial-ShareAlike 4.0 License](https://creativecommons.org/licenses/by-nc-sa/4.0/), which allows others to remix, tweak, and build upon the work non-commercially, as long as appropriate credit is given and the new creations are licensed under the identical terms.

For reprints contact: reprint@ipinnovative.com

1. Introduction

Though deep brain stimulation (DBS) is a well-established minimally invasive gold standard therapeutic surgical procedure, pinpointing the sites of the organs and accurately implanting the leads and microelectrodes is must.^{16,41,42} But other factors also play an important role, and at times anatomically^{17,18} and physiologically⁶ ideally embedded electrodes do not provoke reasonable motoric enhancement following neuro modulation. Such heterogenous findings

among subjects show trials in perfect subject choice for the treatment, so, a need exists for more evaluation tools and utilities accurately.

The age-old levodopa (L-dopa) is still used and regarded as standard medicine plus reliable candidates for DBS.¹⁰ Latest imaging, radiomics, bio chemical analysis of blood and cerebrospinal fluid techniques enables scientific-research technical for deeper estimation of disease plus explicit clinical/experimental results predicting biomarkers

*Corresponding author: Venkateshwarla Rama Raju
Email: drvenkateshwararr@gmail.com

discoveries.⁵ Resting-state functional magnetic resonance and diffusion tensor imaging for brain functional connectivity are explored as possible DBS outcomes predicting properties.^{14,15} Speedy development of open source followed by user-friendly texture feature (radiomic) tools and utilities are employed to detect the Parkinson linked disease radio ‘genomic-features’, also enables researchers to analyze patients’ radio logical data as of a special prospect For several years degeneration of dopaminergic chemical messenger cells within the substantianigra (SN) spotted as central point for symptoms (both cardinal motoric and non-motoric).^{3,4} The current evolution of radiomic studies for unique brain diseases and neuro degenerative disorders oversaw to PD, however, greatly to cortical, sub cortical anatomical - structures and motorcortex too.¹⁹ Newly it is detected that SN sensitivity (susceptibility) characteristic-features from radiomic-textures can foresee overall motor and muscle-stiffness/rigidity outcomes of STN-DBS within PD also proposed an extrapolative prognostic machine learning perfect prototypical model for STN-DBS for choosing the subject.⁷ α (alpha) synuclein is a pre synaptic neural (neuronal) protein, so its anatomical-structural changes play significant role within pathogenesis of neuro degenerative Parkinson diseases.

Recent studies worked on the new archetypal – classic models of Parkinson patho genesis with the α - synuclein origin source-site plus connectome model-simulation, which divides Parkinson disease into two of the sub types: body-first sub type or brain - first sub type.² Consistent with this model as stated by this model, within the body-first sub type, alpha- synuclein pathology presumably originates in the enteric or autonomic nervous system which spreads in the direction of central nervous system(CNS), while the brain primary sub type α -synuclein pathology seemingly instigates within amygdalē (Figure 1, Figure 2, corpus amygdaloideum) or else close anatomical-structures. Thus, dissimilar sub types have distinct medical management of onsets of Parkinson`s. Within vertebrae body - first sub type, the disease begins symmetrically, in proportion, and is contra positive reverse of first sub type of brain.

Thence, it raises a rationale—theory “hypothesis” concerning unique stimulus outcomes with DBS stimulators (implanted pulse generators called IPGs) \forall every Parkinson sub type’. Amygdalē is one—of the two “almond-shaped” clusters-of-nuclei situated medially deep in the ‘temporal-lobes’ of human-brain’s cerebrum within intricate-spinal. Its means for memory-processing, making the decisions, decision making, as well as responding to emotions, i.e., “emotional-responses”, which includes panic, anxiety, aggression, trepidation, nightmares, terrors, etc.. It is a segment of the “limbic-system” and termed in 1822.⁴⁰

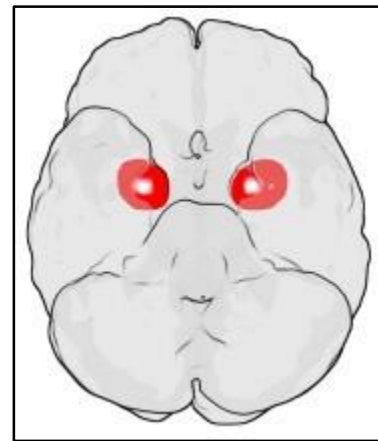


Figure 1: Site of amygdalē in the brain

The sub slices of amygdalē is shown in **Figure 2**.

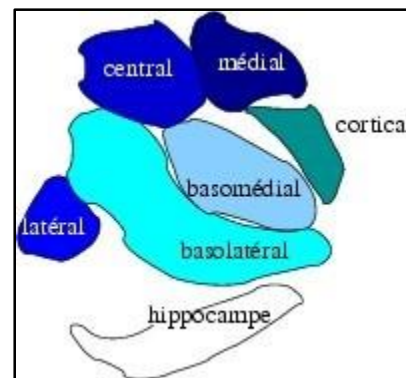


Figure 2: The sub slices of amygdalē

Substantial innovative developments attained in the artificial intelligence machine- learning (ML)based radiomic-textures in current years, sought at upgrading the intelligence of brains neurological disorders and diseases plus defining and also shaping the maximum choices of effective medical diagnostics treatment, clinical and/or diagnosis. Merging the abstraction of “radiomics texture-features” thru these techniques will cater green non - invasive bio markers representing the diseased and recovered subjects class, plus foster a restored detection of stimulus candidates.^{8,12} At the movement, we postulate or theorize that pre op image radiomic-texture exploration and investigation of the amygdalē-hippocampus area zone (patho-physiological locations), might aid and differentiate the subjects who have had advantage greatest as of the DBS surgery for implantation of the electrodes and pulse-generators around the STN. Textures of amygdalē or else adjacent anatomical-structures might function as hypothetically latest prognosis predicting image bio markers for management plan. So, our objective is to evolve radiomic-texture model simulation so as to predict outcome of motor in Parkinson`s with subthalamic-nuclei deep brain stimulators.

Further, the use of bio markers in heterogeneous cancer-malignancy cells, neurodegenerative Parkinson disease subthalamic-nucleus neural (neuronal) cells and pallidal neurons have led to the concept of personalized medicine for diseased conditions (patients). Personalized medicine offers finer prognostic-diagnosis plus managerial-treatment choices accessible to clinicians. Radiological images plan a chance to save and distribute distinctive (unique) data on 'unique-types' of tissue. Yet, acquiring valuable information from all "radio-logical-data" is tough in the 'bigdata' era of genomics and phenomics. Latest improvements in computational power plus application of bigdata of genomics have generated a new area of research termed "Radiomics means feature-pattern textures". It's defined as optimum throughput abstraction of finite-variable image features or textures or feature-manifestations from image to decode/encode encrypted tissue pathology, and also establishing a higher dimensional data set for extracting features. The features supply data/information on the 'gray-scale patterns', 'inter-pixel relationships'. Also, contour, spatio spectral nonlinear dynamics and dynamical-mechanisms plus properties can be obtained in the like zones of interest over radiology images.

Similarly, these feature-manifestations can be employed to evolve computational simulation models and statistical modeling and real-time (multi-channel) prototype models with advanced artificial intelligence based unsupervised machine learning algorithms which can aid as tools and utilities for custom-made (personalized and tailored) adapted diagnosis also behavioral-treatment direction.

2. A Brief Historical Perspective on Radiomics

Radiological image systems are able machine tools applied for finding, discrete attributes (or entities) within the diseased subjects' conditions, namely, computed axial tomography (CAT or CT) MRI/f-MRI, PET and ultrasound. They establish dissimilar tissue differentiations entrenched whether matter, i.e., organ of the brain is 'typical' or 'atypical'. These mechanisms are employed by electro neuro-radiologists to detect patterns (or 'signatures') to reach out to infer the diagnosis. So that the findings are diagnosed and discover the cause. It is said that when a system is working properly what do we do we often ignore it however if there is any malfunction then it has to be diagnosed and discover the cause.^{41,42} Image consists of information content its clarity is inconvincible and invisible to the clinician's eye and so this subtle yet hidden information initiates and creates a "radio logical texture" which gives considerable information coupled with the 'tissue-of-interest' than hitherto believed or supposed. Hence, the theory of hypothesis of "Radiomics" was introduced as a novel method to find and then change or transform the metrics (system of measurements) achieved by using texture (radiomics) plus further supplementary testing techniques upon radio logical and image matrices. Even so, it's a novel application employing determined methods, precisely, discriminant, clustering, texture, coherence,

cogent, entropy, haralick, average amount of mutual information plus some further features.¹⁹⁻²³ The unique part of radiomic-textures is similarity of these portions to alternating end points also the beginning of risen machines and machines computational complexities potentially accessible currently. The central theory after texture-radiomics is that the information is underlying inside the radio logical images can be mined by employing sophisticated 'radiomic-textures' and phase(shape) angle and size of tissues analysis. As of this elicitation and evocation of the data, 'higher-dimensional-space' is established. Automatically, radiomic-texture is employed by all to derive attributes any visual or trace. Radiomics, i.e., radiomic-textures techniques was derived as of information theory coding.^{19,20} Later, statistical variates and measures were amended and then incorporated to integrate ashen (gray) matrices and matrix—operations to perform over the input(i/p) data.^{20,24}

Though radiomics was applied in "aerial-photos",⁶ later on it was applied in medical imaging.^{20,27} Now, texture (radiomic) features are applied in several special areas and fields of research, remarkably, thru enhanced complex computational capacity, computational time and space (storage) and asymptotic complexities, and on and offline 'digital-storage' capacities.²⁰⁻³¹ Furthermore, given the 'region-of-interest' ('R.o.I'), the phase-angle ('shape based') feature—manifestations can correspondingly be obtained in consort with, together with radiomic-texture inferences.²³

Thru the newly added skill of computer machinery and technological knowledge to decrease computational complexity obsessed by analyses of applying radiomic-textures, the phase (shape) inferences, which led to the growth of innovative area-of-research called "Radiomics" which is defined as the maximum amount of the throughput extraction of quantifiable features from radio logical images making a higher dimensional dataset ensuing datamining aimed at possibly better 'decision-support'.³⁰⁻³⁹ But radiomic is depending on "texture", phase, i.e., "shape" plus "grey-level statistics" inside the images towards determining numerous connections linked to "clinic-pathological-data". Yet the 'correlation' to real and valid natural biologic and genetic implication is must. However, using radiomics (texture-features) in image-analysis, it's viable to decode/encode and decrypt and/or encrypt "tissue-pathology" which is invisible to the neurologists neuroradiologists visualization.

In what way this is feasible? The lesions, tumors, the abrasions, etc., are spatiotemporally varied and might be sampled lower in 'medical-management processes, for instance, in surgery (tissue-removal). Thus, entire lesion is uncharacterized, which is 'unfavorable/detrimental', negative and disadvantageous to determine curing and therapeutic alternatives. So, this limitation can be hypothetically overwhelmed thru radiomic-method and is able to obtain 'variable-features, computable-features' within

lesion and findings might equated to lesions pathological outcome or-else additional data info, for instance, existence or endurance.³²

This research study predicts subthalamic-nucleus outcome of Parkinson patients' disease stimulations with DBS stimulators by applying the radiomic techniques such that quantifiable image and/or signal-features' or textures extrapolated from pre op magnetic resonance imaging. This also outlines historical-perspectives, mathematical-frameworks, plus some latest 'applications-of- radiomic procedures to discover lesion and/or tumor features also proves "radiomic-textures" are capable tools in clinical and/or diagnostic clinic—statistical applications. Also, this study will yield an outline of state-of-art techniques, skill-of-radiomic textures for several lesions like STN, cancer-tumors. Finally, we conclude the viewpoint over the likely on "future-of-radiomics" and texture- features within the "personalized medicine" therapies, and therapeutic-processes.

3. Methodology

3.1. Parkinson's subjects

Thirty-four Parkinson subjects (Parkinson diseased patients) were recruited in this study. Subjects with advanced PD of >5 years with good response to L-Dopa and H and Y score of <4 with normal cognition were eligible for surgery. Surgery was planned by applying a CRW frame with an MRI protocol using a sophisticated Frame link computer software with 5 channels and intra operative microelectrode recording. Micro electrode recording was performed in all subjects extending

±10mm (above and below STN target levels). Ultimate target choice was based on dyskinesias of induced macro stimulus plus proven by post op MRI. Subjects underwent DBS implantation at STN site.

5 subjects (5~5%) showed mean DBS motor outcome. 9 amygdalē-nuclei plus 12 hippocampus 34 subfields were segmented with Free surfer 7.0 version pipeline from pre op MRI. An "Py-Radiomics" platform running under free surfer operating system-software was employed to extrapolate 12 0texture ('radiomic-features') for every nucleus and sub field ensuing in 5,040 feature-manifestations. The m.R.M.R feature-selection technique was employed to reduce the number-of-features to 20, 8 AI-based ML techniques: normalized-binary logistic regression (LR), decision tree classifier (DT), naive Bayes classifier (NB), kernel support vector machine (SVM), feed-forward neuronal network-based auto encoder for anomaly detection (DNN-A) were applied to build the models for poor v/s. good and very good STN-DBS motor outcome prediction. There were clinically and demographically no differences amongst 2 cohorts (Table 1).

For optimum lead-point (access) in the (motor) region of subthalamic, target 2mm is chosen as of 'medial-border' at the 'maximal- rubral' length as.¹ Stereo tactic functional post op MRI was applied to check precise lead-position. PDC scale scores were computed pre op 180 days following insertion of IPG electrodes. PDCS score progression for >30% was deemed ('good' or 'very-good' result of stimulus).

Table 1: Parkinson's clinical characteristics radiomics

Attributes/ Entities	Meagre/poor outcome of DBS (underprivileged)	Decent/better outcome of DBS	p-value
# of PD subjects	5	29	-
Age-of-diseased	63(60 - 68)years	60(57 - 62)years	0.261
Sex	Masculine: 4(80%) Feminine: 1(20%)	Masculine: 12(41%) Feminine: 17(59%)	0.163
P.D.C.S. pre op	P.D.C.S. post op	22(18 - 27)	0.608
P.D.C.S. post op	18(16 - 27)	11(7 - 16)	0.034
L.E.D.D. pre op(mg)	710(620 - 840)	720(620 - 800)	0.980
L.E.D.D. post op(mg)	710(600 - 840)	300(300 - 420)	<0.001
Dislocation of D B S	0.2(0.0 - 0.5)	0.3(0.0 - 0.5)	0.602
Electrodes,(mm)			

Stage(age), pre op score of PD composite-scale('PDCS'), Post of 'PDCS', pre op l-dopa-equivalent daily- dose('LEED'), post op 'LEED', 'electrode-movement' are Stated as 'median', 'interquartiles'. Chi-square χ^2 -

Test1 = 1.256, Fisher's-test (statistics) 5.667, Chi-square χ^2 -test1=0.261, Chi-square χ^2 -test=4.491, Chi-square χ^2 -Test = 0.001, Chi-square- χ^2 -test1=11.662, Chi-square χ^2 -test=0.271.

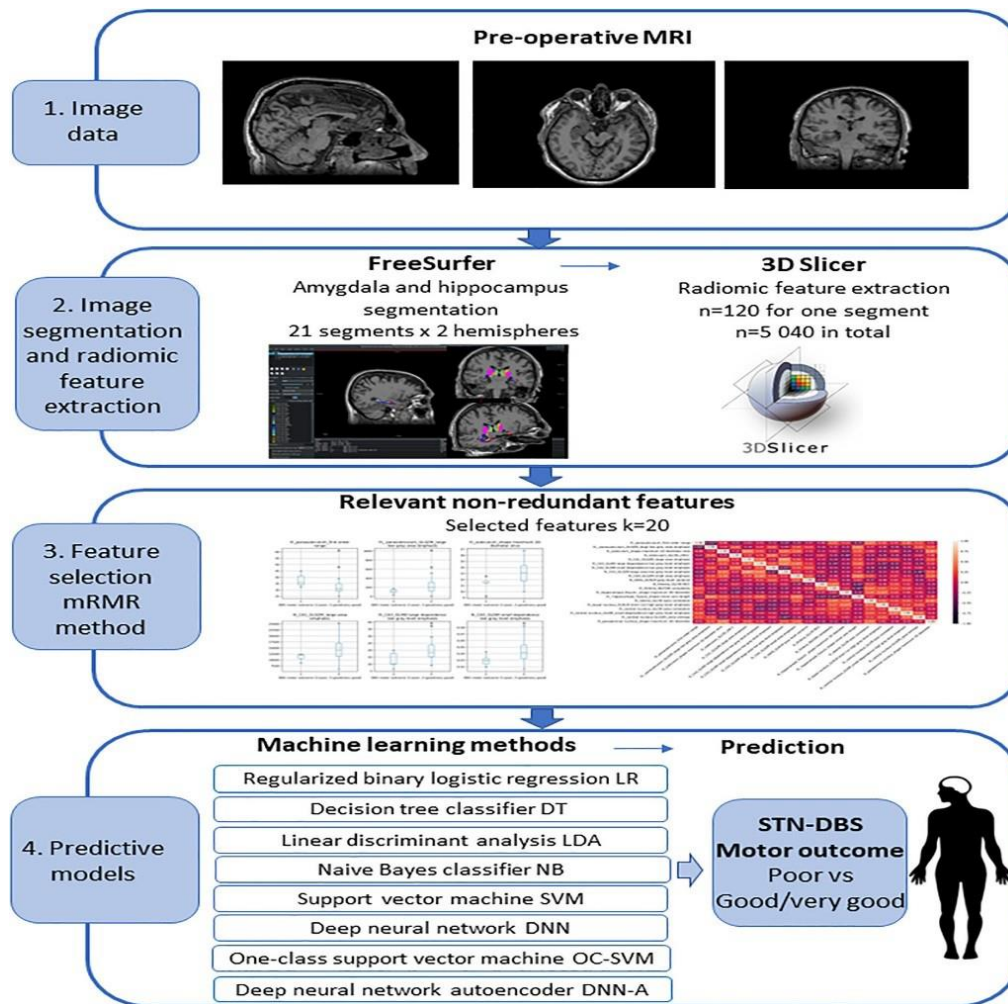


Figure 3: Planning: data and system flow functioning of pre op estimate of stn – dbs in parkinsons. 1. A. Pre op MRI data acquisition with 7T, 2. B. Amygdalē plus hippocampus separation by Free-Surfer, C.Textures (radiomic-feature) extraction with 3Dimensional- slicer, 3.C. Texture-selection with m.RMR technique: D. important features chosen, E. Non-redundant-features chosen ($k=20$), 4. Prognostic models of ML, F. LR, DT, LDA, NB, SVM, DNN, OC-SVM, DNN-A, G. Estimation of stn-neurons with dbs and its result is poor v/s. good or very-good.

3.2. Preprocessing of image acquisition and separation

Pre op T1 and T2 weighted images were employed in free surfer-module version7.0 aimed at programmed brain MRI morphological/morpho-metric ‘data-extraction’ as well as segmentation also sub regions of amygdalē and hippocampus.¹³ (Figure 3) The Free surfer amygdalē-hippocampus pipe-line technique (with transputer-based reduced instruction set computers (RISC) and CISC complex instruction set computers) separated sub regions of amygdalē-hippocampus concurrently evading imbrication plus generating 12 hippocampus sub divisions, 9nucleus of the amygdalē.(Table 2) For every hemisphere (left and right hemispheres of brain), 21 segments got obtained, in total some of 42 segments were achieved (Figure 1A,B).

3.3. Feature—extractions/ textures (radiomics)

The amygdalē-hippocampus free surfer separation data-files were employed for every subject. The texture features were

done with open-source operating system running under “Py-Radiomics” platform.¹⁴

As an addendum, add on extension (radiomic) for 3dimensional/rotational slicer was retained aimed at texture(radiomic) ‘feature- extractions as shape (phases, i.e.,26 shapes), first-order, gray-level co-occurrence matrix(GLCM 24), 19first-order textures, 16Gray Level Run Length/coding Matrix (GLRLM) feature-manifestations, 16 Gray Level Size Zone Matrix (GLSZM) manifestations, 14 Gray Level Dependence Matrix (GLDM) textures, followed by 5Neighboring Gray Tone Difference Matrix (NGTDM) textures. The method labelled given 120 radiomic (features) representing every 21 Slices in brains left-hemisphere and right-hemisphere, 5040 texture-features altogether (see Figure 1. ‘C’).

3.4. Feature-sections of radiomic-textures

For this what we did was, we have applied the m.R.M.R method ([20]), such that, it successfully lowers the unwanted feature-manifestations but limiting the ‘significant- features’

for machine-learning prediction simulation prototype models (Figures 1D,E). Since the aim is to distinguish subjects into two types of impoverished (deprived and disadvantaged) v/s better/best outcome of DB stimulator (stimulations to STN), the features which have most significance and application concerning the type (or class) estimate were governed thorough the analysis of variance (“one—way ANOVA”) Fisher’s test (‘F-test). Unwanted textures were defined through the correlation (Pearson’s) by applying the following formula (equation).

$$r = \frac{\sum (x_i - \bar{x})(y_i - \bar{y})}{\sqrt{\sum (x_i - \bar{x})^2 \sum (y_i - \bar{y})^2}}$$

Where, ‘r’ is the correlation-coefficient (of the Pearson’s), x_i is the values of variable ‘x’ within the sample. \bar{x} is the mean of values of variable ‘x’, y_i is the values of variable ‘y’ in a sample. \bar{y} is the mean of values of variable ‘y’.

The ‘best sub-set’ of 20 features was formed by choosing the important textures whilst restricting for the unwanted components contained by the chosen (opted) textures. The textures were chosen and by taking into a tiny sample-size of Parkinson’s (N = 34) plus pointing and then targeting to steer clear of fitting exaggeratedly. However, it can be noted that the sample – to texture fraction must be and utmost at best ≥ 2 .¹¹ The noise and low-ratio outcomes in prototype simulation/model— fitting of data as well as detection is poor and precision too once used to invisible or unnoticed data-elements.

3.4. Prediction of Feature-based ML in sub thalamic nuclei for DBS outcome

Following the significant textures, we then employed those textures to create the models for the result of DBS on STN estimate (see **Figure 1**. ‘F’ and ‘G’). Some of the machine learning techniques applied in this study are:

1. Normalized/standardized (are also said to be recognized) binary logistic-regression (LR) thru “sigmoid-function”. Note: The normalization designate is identical to the sum of squares (SoS) of all the ‘feature-weights’.
2. Decision-tree classifier (“DTC”),
3. Linear discriminate analysis (“LDA”)/latent variate factorial (or factor) analysis.^{33,34}
4. Naive Bayes—classifier (“NB”),
5. Kernel support vector machine (SVM) through the Gaussian “ radial- basis” function as a “kernel-function”,
6. Deep feed-forward ‘ NN’ (“DNN”), the network (NW) had 2 hidden-layers together with 11, 7 neurons followed by the Re-LU ‘transfer-functions’, correspondingly, plus 1 neuron beside “sigmoid-activation function” within the layer output (o/p).

7. Drop out algorithm was utilized to set as a chance or randomly, a ten 10% proportion of detectable plus suppressed or unknown neurons to 0 throughout preparation to circumvent over fitting, ‘back-propagation’, i.e., ‘error-back’ training technique together with adaptive moment and action approximation was employed.
8. The support-vector-machine (i.e., “a one class OC-SVM”) through Gaussian ‘radial-basis’ function as a kernel ‘- function’. The adverse and undesirable o/p shows the low density of studies also the findings with in the discovery of irregularity, which means that the remark which differs as of the lead of data notably; insignificant results by deep brain stimulations to the sub thalamic nuclei is considered incongruity or irregularity.
9. Deep feed-forward NN-based auto encoder (DNN-A) aimed at irregularity uncovering. The encoder (and decoder) contained of i/p layer plus 1 hidden-layer together with 18 neurons also “Re-LU transfer-function”, the hidden-layer consisted of 4 neurons together with “Re-LU transfer function”, the encoder was shaped of 1 latent - layer together 18 neurons plus Re-LU’ transfer-function also o/p layer through 20 neurons followed by “linear-transfer function”. The drop out procedure was used to set a 10% portion of percentage of observable and latent neurons to 0. The back- propagation/ (‘error-back’) procedure by adaptive action/movement approximation was employed.

Irregularity was detected if error of rebuilt 20 DMs “feature-vector” was superior with 1 SD than MSE of the rebuilt samples as of the type of decent (upright) and better (very-good) result of motor outcome with stimulations.

The data was segmented to tests sets. NNs training-set contained 85% (V the data-set, 4 as of the type of meagre results (STN - DBS of motor, 24 as of the type of “good”, “very-good”, plus lingering 15% of data has applied to examining the test (1, 5 as of every-class-type). Before the analysis, the data sets were normalized with normal scalar-quantity. Test data followed by NN-training data was strapped by 1000 repeats, gaining test data continually through alternative as of the accessible and existing ‘data-set’. For equalizing the unequal data size sets, the type - of -class weights were likely guessed and also employed in AI-ML techniques. The parameters like ‘ precision’, ‘ specificity’, ‘ sensitivity’, and ‘ area’ of ‘ receiver operating characteristic’ (‘R.o.C’) curve (‘AUC’) of AI-ML mathematical frameworks and prototype-models were projected also be an average-of-over 1000 boot strapped reiterations.

Texture (radiomic) feature-selection, data-processing, plus AI-based ML techniques were run and executed through “Python” software and framework.⁹

Table 2: Labeling of free-surfer’s amygdalē-hippocampus separation out/put (o/p) plus nucleus thru chosen features (radiomic) applied to foresee stimulus-outcome of STN motor (sub fields of nucleus)

Amygdalē		Hippocampal	
Nucleus	Textures (radiomic-features)	Sub sections	Textures (radiomic-feature)
Basal-nuclei(BN)	GLRLM short run high gray	Parasubiculum	First-order-range,
Level emphasis	GLSZM larger minimal grey region	-	-
Lateral-Nuclei	GLCM ‘auto-correlation’	Presubiculum	-
Auxiliary BN	-	Subiculum	Shape maximum 2D diameter slice, GLCM IMC1
Anterior	-	CA1	GLSZM large area emphasis
Amygdalēid-nuclei			
Central-nuclei	GLCM auto correlation	CA3	GLDM enormous dependency
	GLDM minor dependency extreme grey smooth stress, GLSZM ‘entropy’-region/zone		GLDM enormous dependency GLDM enormous dependency GLDM small dependence little grey-level stress, GLSZM sizable region small
M e d i a l	-	CA4	GLSZM-tiny region importance
Cortical	-	GC-ML-DG	-
Paralaminarl	Form/shape most 3DMI	‘Molecular-layer	-
Cortico	-	H A T A	GLRLM gray level variance
Amygdalēid			
Change-area (transition - region)	-	Fimbria	GLCM,MCC,NGTDM difficulty
		Hippocampus-train	-
		Hippocampus-crevice	Form most 3DM width, Sliced-shape(fissures)small ‘axis-length’

4. Results

Amygdalē plus hippocampus zone selections, texture-feature extractions’ were caused to identify 20ut most at best texture features which signify amygdalē basal, lateral, central, paralimar, hippocampus para-subiculum, and subiculum nucleuses, as well as C A1, CA3, CA4, HATA, fimbria, hippocampus – fissures’. 20 textures (radiomic-features) were designated over the 5040features which were extracted with m-RMR procedure.

The findings with the motoric stn – dbas outcome in those 20 textures (radiomic-features) allocations chosen within the type-classes of modest (“Good V/s. Good/Very-Good) are shown in **Figure 2**. This illustration neatly, clearly and legibly demonstrates the variation with in medians of textures in the 2 cohort-groups. The changes in allocations or allotments are important clinic-statistically \forall texture - features (Kruskal Wallis H- test with 2 degree of freedom, $p<0.03$, statistically significant) plus verify the utmost at best greatest application and importance regarding the ‘motoric-outcome’ predictively-estimate. The Spearman’s ρ

–correlation-coefficients among the textures alter as of from –0.48 to +0.49 plus explain and prove relative, pale (low) or no correlation justifying the smallest laying-off.⁵

All those chosen textures were utilized to prognose the dbs outcome versus (v/s) 2 cohort-groups outcome, which means to classify to detect the problems within post opstn - dbs motoric performance. The precision, specificity, and understanding the feeling-sensitivity’ plus A U C of ML techniques/procedures and processes are generated (and depicted) in **Table 3**, however the curvatures of R o C plus A U C are explained jointly in **Figure 4**.

4.1. Processing sub thalamic nucleus data

The dataflow and system flow (“work - flow”) model processing of MR images, amygdalē and hippo campus separation/ (‘segmentation’), texture ‘feature-extractions’ by radiomics technique, assortment, application of AI intelligent machine learning techniques aimed at post op prediction of sub thalamic nucleus (motor) outcome using the deep brain stimulations is illustrated in **Figure 5**.

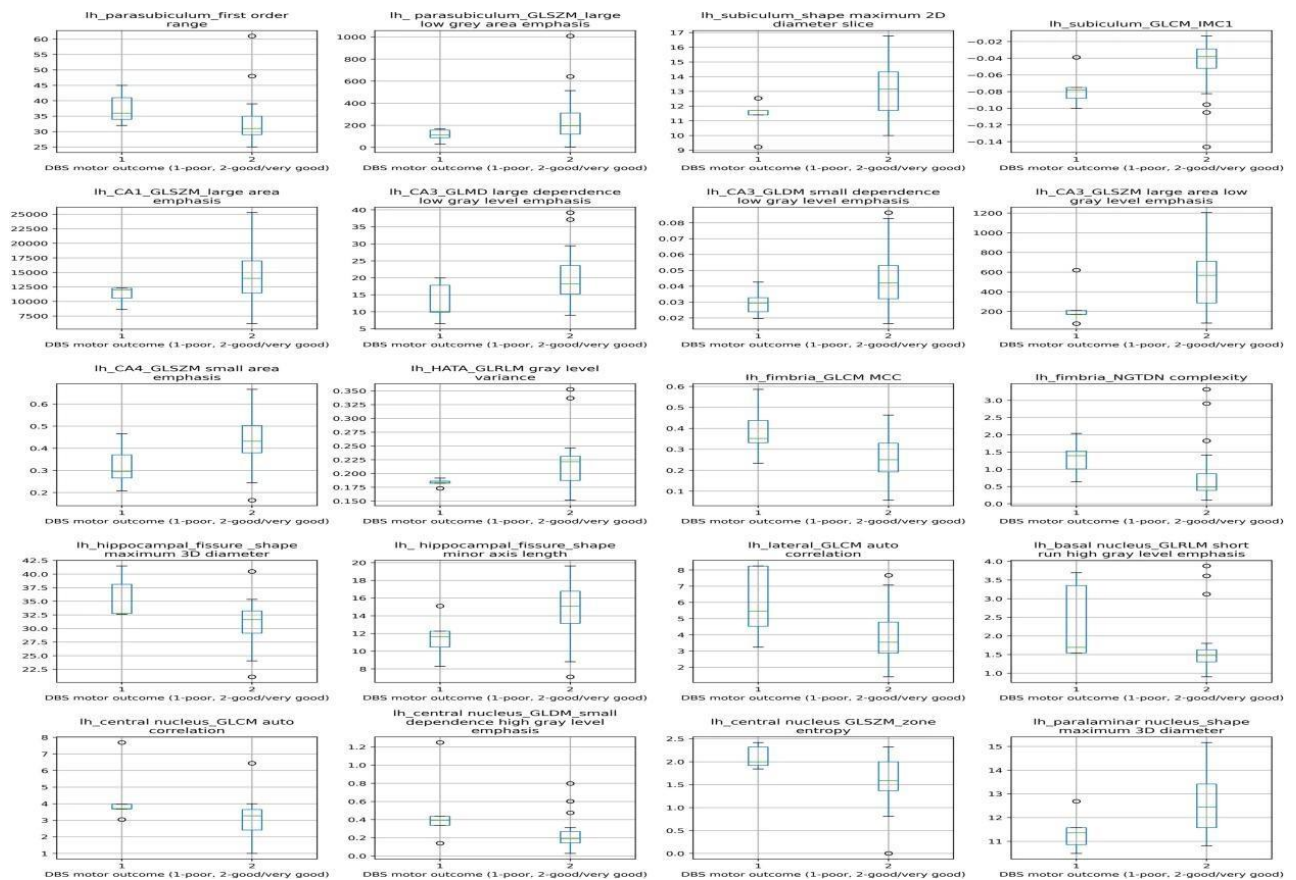


Figure 4: Differentiating amongst weak S T N – D B S result plus virtuous/very-good(better) STN –DBS result representing 20chosen textures(‘radiomic-features’). Disseminations-of-features amid 2 cohorts of STN – DBS vary statistically($p < 0.05$, significant), Chi-square-test χ^2 plus ‘p’-value (in digressions): *lh* – parasubiculum 1st order-range: 4.402(0.036), *lh* –parasubiculum GLSZ Big small grey region importance: 3.878(0.049), *lh* – subiculum-phase (shape) max 2Dmdiameter-slice: 3.980(0.046), *lh* subiculum GLCM – IMC 1:4.682(0.030), Code *lh* at the feature-label shows brains left-hemi-sphere.

Table 3: Precision, ‘sensitivity’ and ‘specificity’, A U C of AI-ML techniques and procedures` used within the post op STN – DBS result (‘motor-outcome’) prediction using 20 selected features.

#.	Method	Precision Sensitivity	Specificity	Area under ROC
(AI-ML))	(%)	(%)	(%)	(AuC)
Normalized-binary	96.60±7.24	99.30±8.34	96.12±8.60	0.98±0.06
Logistic-regression(L R)				
Decision-tree-classifier(D T)	77.42±12.50	14.60±35.33	89.98±14.15	0.52±0.18
LinearDiscriminantAnalysis(L D A)	77.90±18.30	83.20±37.41	76.84±19.64	0.80±0.22
Naive “Bayes-classifier” (N B)	86.62±7.27	21.90±41.40	99.56±3.07	0.61±0.21
Support-vector-machine(S V M)	91.72±04	60.40±48.	93 97.98±6.03	0.79±0.24
Deep feed-forward-neural NN(D NN)	87.25±4.80	86.60±34.08	87.38±17.48	0.87±0.18
One-Class-SVM (‘OC-SVM’)	63.33±17.90	24.40±42.96	71.12±20.70	0.48±0.23
Deep- N N -autoencoder(DNN - A)	70.73±10.70	73.36±11.60	68.10±22.90	0.71±0.11

Old faced-values show the largest precision.

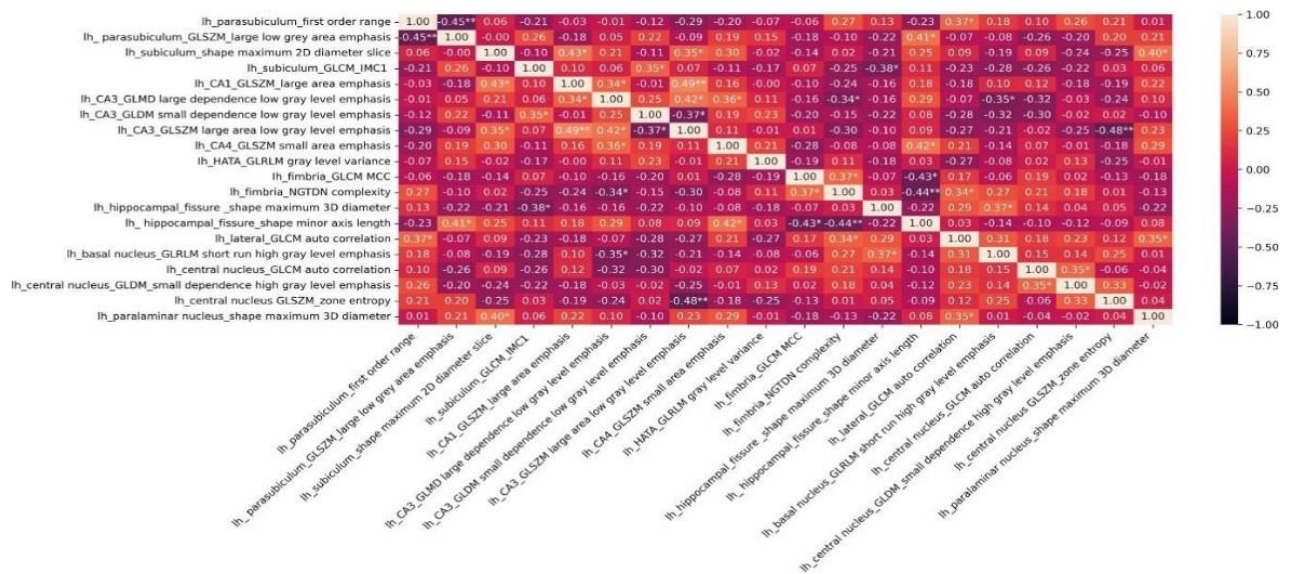


Figure 5: Heat map of Spearman's ρ correlation-coefficients of 20 chosen textures ('radiomic- features', $*p<0.05$, $**p<0.001$ explain meaningful "associations/correlations".

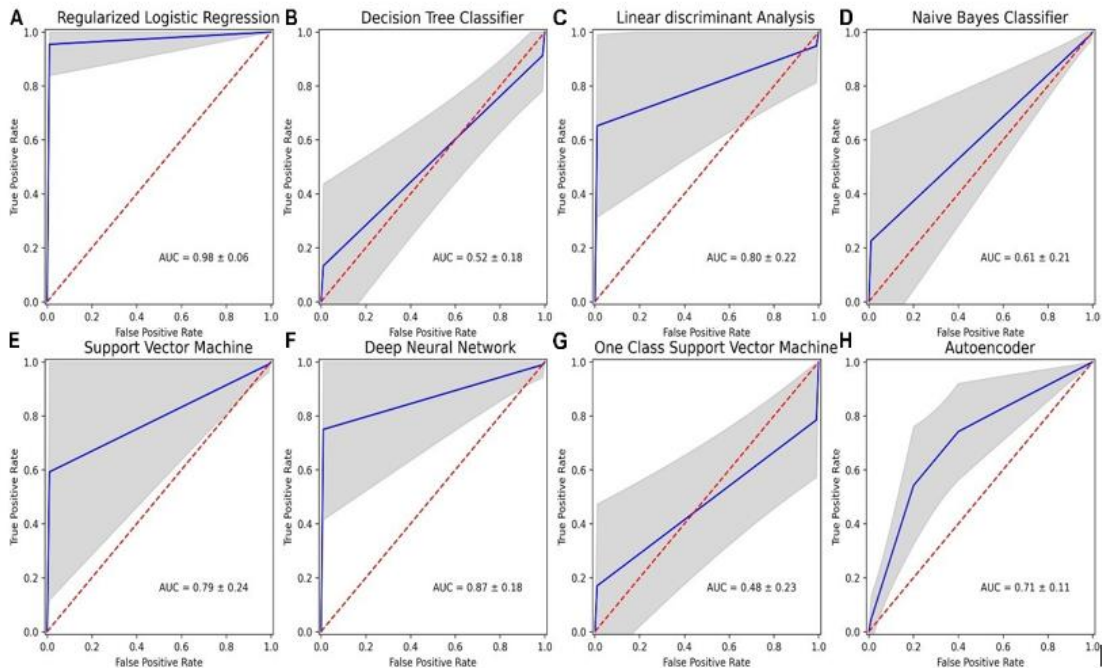


Figure 6: The R O C arcs/curvatures aimed at ML techniques (strategies and processes through computation) used in post -op STN – DBS results of “motor-outcome prediction” through the 20 chosen-radiomic-texture features: Fig 6.A. Normalized-binary logistic-regression (LR), 6.B. Decision-tree- classifier ('D T'), 6.C. LDA, 6.D. The simple (naïve) Bayes-classifier (N B), 6.E. The “kernel-support vector- machine” (“SVM”), 6.F. Deepfeed-forward NNW (DNN), 6.G. One-class SVMs (OC-SVMs), 6.H. Feed-forward NNW-based auto encoder aimed at abnormality discovery DNN - A. An average of R O C is depicted within blueish, the SD is denoted through grey region. A scattered ‘red-line’ signifies likelihood probability exhibition/presentation, arcs (the curvatures) which vary further in the direction of the ‘top-left’ characterize respectable likelihood estimates.

Soft (depleted) sensitivity plus depleted A U C for detecting the inadequate results of s t n d b s were achieved by applying the “ DT- classifier”, precision: $77.43 \pm 12.55\%$, sensitivity: $14.60 \pm 35.34\%$, specificity: $\sim 9.00(89.99) \pm 14.15\%$, AUC: 0.52 ± 0.18 , “NB-classifier” whose precision is: $86.62 \pm 7.27\%$, sensitivity: $21.90 \pm 41.38\%$, specificity: $99.56 \pm 3.07\%$, AUC: 0.61 ± 0.21 , OC-SVM:

precision is $63.33 \pm 17.88\%$, sensitivity: $24.40 \pm 42.97\%$, specificity: $71.12 \pm 20.65\%$, AUC: 0.48 ± 0.23 . The “DT- tree classifier” is based on ordered (i.e., hierarchical) sequence of results on the texture- features which is susceptible to tiny differences with in the ‘ NNW training- set’, exclusively meant for such intricate data in higher- dimensional- texture (features) space as’ radiomic-texture events or measurements. (Figure 6)

The N B- classifier thinks that the texture (radiomic - features) is free plus squared (derived) as of with “Gaussian-distributions” (bell shaped curves and maximum peak at the turning points), and unrelated within this study. The ‘OC – SVM’ finds the abnormalities (motor functioning results of with STN-DBS) while data outside the gain knowledge of outcome border line of usual standard cases: Good / Very Good result with stimulations. The vector machine can also establish complicated limitations in higher “dimensional-feature-space” plus it is not as much of liable to over fitting lead to in inadequate precision.

Reasonably respectable execution was acquired through “LDA (‘precision: 77.90±18.28%, ‘sensitivity: 83.20±37.41%, ‘Specificity: 76.84±19.64%,’ AUC: 0.80±0.22, precision of DNN-A: 70.73±10.68%, ‘sensitivity 73.36±11.60%, ‘Specificity: 68.10±22.91%,’ AUC’ 0.71±0.11, plus S V M precision: 91.72±9.04%, sensitivity: 60.40±48.93%, specificity: 97.98±6.03%, AUC: 0.79±0.24). The L D A does not succeed to separate non linearly discrete type-classes which yields very high flexibility of sensitivity because of heterogeneousness or conglomeration of array of the data.

5. Discussion

The DNN - A presented high compassion, which means the restoration—error of the obtainable inadequate results with DBS of STN microelectrode recording (MER) data was great signaling that the samples-data was an abnormality. Conversely, owing to an intricate D N N - A construction a reasonable (medium) fraction of decent plus better D B S of STN samples were furthermore rebuilt by extreme error’s, lead to in diminished-specificity’. Support vector machine explores aimed at the linear best splitting hyper plane within the altered ‘feature-space’ with “support-vectors”, that is the data-points nearest to the hyper plane as of 2 types-of-classes. In this study, the procedure stands and experiences as of an excessive and extreme data set plus benefits a type-class by a substantial amount-of the samples.

Since the DBS of STN 2cohorts outcome is high hence support vector machine yields extreme specificity plus minimal sensitivity. The highest overall prognostic precision scores were attained thru standardized binary- L R (precision: 96.65±7.24%, sensitivity: 99.30±8.34%, specificity: 96.12±8.60%, “A U C: 0.98±0.06) plus.

The D N N-precision: 87.25±14.80%, ‘sensitivity: 86.60±34.08%, specificity: 87.38±17.48%, “A U C: 0.87±0.18). The binary L R needed only some more parameters to be projected plus was normalized to prevent over fitting, hence causing in extreme sensitivity plus specificity through the small-variance.

Even though, the D N N concert has great erraticism-variability or inconsistency in compassion owing to deep neuronal net-work (‘NNW’) construction also incomplete

model- size, the attained precision is auspicious also demonstrates the potential of “D N N” proposal in classifying meagre S T N – D B S findings. In machine learning unfair data sets cause distinguished mainstream criterions so in the study (mainstream criterion=85.29%). The regression plus the D N N surpass this limit, prove extreme ‘sensitivity’ plus ‘specificity’, thus the approaches may be studied appropriate for resolving the stated issue. Our findings show that the mission of outcome S T N – D B S likelihood is intricate, plus implies numerous strides as texture (radiomic) ‘feature-extraction’ as of the images, ‘feature – selection’, the prototype-model growth plus guidance, plus precision assessment. The ‘higher-dimensional’ radiomic (texture) ‘feature-space’ plus restricted ‘sample-size’ need getting a trade - offs amongst artificial intelligence-based machine learning difficulty plus its execution.

6. Conclusion

Our findings demonstrate that the capability and the potential of amygdalē as well as hippocampal texture (radiomic) feature-manifestations (of motoric symptoms) towards predicting the deep brain stimulations outcome when stimulated to sub thalamic nucleus in Parkinson’s. However, amygdalē followed by hippocampal radiomic-variations ought be investigated on largerscale aimed at their significance in Parkinson’s range intended for the deep brain stimulations to sub thalamic nucleus. The radiomic (texture) characteristics on the degree of amygdalē influence disclose scientific-pathos logical, and medical management residues (accumulations) of the α – synuclein. Yet, correlation of texture (‘radiomic’) cardinal motoric manifestations through immune histo chemical Parkinson’s data and information are critical and fundamentally aimed at our scientific-rationale/‘hypothesis’ proof and therefore can be postulated.

7. Ethical No.

Nims/2019/02/vrr.

8. Source of Funding

None.

9. Conflict of Interest

None.

References

1. Bejjani BP, Dormont D, Pidoux B, Yelnik J, Damier P, Arnulf I, et al. Bilateral subthalamic stimulation for Parkinson’s disease by using three- dimensional stereotactic magnetic resonance imaging and electrophysiological guidance. *J. Neurosurg.* 2000;92(4):615–25.
2. Borghammer P. The-synuclein origin and connectome model (SOC Model) of Parkinson’s disease: Explaining motor asymmetry, non-motor phenotypes, and cognitive decline. *J Parkinsons Dis.* 2021;11(2):455–74.
3. Colpan ME, Slavin KV. Subthalamic and red nucleus volumes in patients with Parkinson’s disease: Do they change with disease progression? *Parkinsonism Relat Disord.* 2010;16(6):398–403.

4. Damier P, Hirsch EC, Agid Y, Graybiel A. The substantia nigra of the human brain: II. Patterns of loss of dopamine-containing neurons in Parkinson's disease. *Brain* 1999;122(Pt 8):1437–48.
5. Hustad E, Aasly JO. Clinical and imaging markers of prodromal Parkinson's disease. *Front Neurol*. 2020;11:395.
6. Koirala N, Serrano L, Paschen S, Falk D, Anwar AR, Kuravi P, et al. Mapping of subthalamic nucleus using microelectrode recordings during deep brain stimulation. *Sci. Rep.* 10:19241.
7. Liu Y, Xiao B, Zhang C, Li J, Lai Y, Shi F, et al. (2021). Predicting motor outcome of subthalamic nucleus deep brain stimulation for Parkinson's disease using quantitative susceptibility mapping and radiomics: A pilot study. *Front Neurosci.* 2021;15:731109.
8. Pedregosa F, Varoquaux G, Gramfort A, Michel V, Thirion B, Grisel O, et al. Scikit-learn: Machine learning in python. *J Mach Learn Res.* 2012;12:2825–30.
9. Pollak P. Deep brain stimulation for Parkinson's disease patient selection. *Handb. Clin. Neurol.* 2013;116:97–105.
10. Raudys Š. "Model selection," in *Statistical and neural classifiers* (London: Springer). 2001:209–66. doi: 10.1007/978-1-4471-0359-2_6
11. Ren Q, Wang Y, Leng S, Nan X, Zhang B, Shuai X, et al. Substantia nigra radiomics feature extraction of Parkinson's disease based on magnitude image of susceptibility weighted imaging. *Front. Neurosci.* 2021;15:557.
12. Sämann PG, Iglesias JE, Gutman B, Grotegerd D, Leenings R, Flint C, et al. FreeSurfer based segmentation of hippocampal subfields: A review of methods and applications, with a novel quality control procedure for ENIGMA. *Hum. Brain Mapp.* 2022;43(1):207–33.
13. van Griethuysen JJM, Fedorov A, Parmar C, Hosny A, Aucoin N, Narayan V, et al. Computational radiomics system to decode the radiographic phenotype. *Cancer Res.* 2017;77(21):e104–7.
14. Wang J, Shang R, He L, Zhou R, Chen Z, Ma Y, et al. Prediction of deep brain stimulation outcome in Parkinson's disease with connectome based on hemispheric asymmetry. *Front Neurosci.* 2021;15:620750.
15. Wang T, Shorran M, Emami A. Towards adaptive deep brain stimulation in Parkinson's disease: Lfp-based feature analysis and classification, in *Proceedings of the 2018 IEEE international conference on acoustics, speech and signal processing (ICASSP)* (Piscataway, NJ: IEEE). 2018:2536–40. doi: 10.1109/ICASSP.2018.8462472
16. Wodarg F, Herzog J, Reese R, Falk D, Pinsker MO, Steigerwald F, et al. Stimulation site within the MRI-defined STN predicts postoperative motor outcome. *Mov. Disord.* 2012;27(7):874–9.
17. Wu Y, Jiang JH, Chen L, Lu JY, Ge JJ, Liu FT, et al. Use of radiomic features and support vector machine to distinguish Parkinson's disease cases from normal controls. *Ann. Transl. Med.* 2019;7(23):773.
18. Zhao Z, Anand R, Wang M. "Maximum relevance and minimum redundancy feature selection methods for a marketing machine learning platform," in *Proceedings of the 2019 IEEE international conference on data science and advanced analytics, DSAA*, Vol. 2019 (Washington, DC: IEEE). 2019:442–52.
19. Shannon CE. A mathematical theory of communication. *Bell Sys Techn J.* 1948;27(3):379–423.
20. Haralick RM, Shanmugam K, Dinstein IH. Textural features for image classification. *IEEE Transactions on Systems, Man Cybernetics.* 1973;6(6):610–21.
21. Galloway MM. Texture analysis using gray level run lengths. *Computer graphics and image processing. IEEE Transact Image Proce.* 1975;4(2):172–19.
22. Amadasun M, King R. Textural features corresponding to textural properties. *IEEE Transactions on Systems, Man and Cybernetics.* 1989;19(5):1264–74.
23. Aerts HJ, Velazquez ER, Leijenaar RT, Parmar C, Grossmann P, Carvalho S, et al. Decoding tumors phenotype by noninvasive imaging using a quantitative radiomics approach. *Nat Commun.* 2014;5:4006.
24. Kaizer H. Tech Note Boston University Research Lab; Boston, Massachusetts: 1955. A quantification of textures on aerial photographs; p. 1955:121
25. Sutton RN, Hall EL. Texture measures for automatic classification of pulmonary disease. *IEEE Transact Comp.* 1972;(7):667–676.
26. Bardeen JM, Carter B, Hawking SW. The Four laws of black hole mechanics. *Commun Math Phys.* 1973;31(2):161–70.
27. Bekenstein JD. Black Holes and Entropy. *Phys Rev D.* 1973;7(8):2333–46.
28. Sonntag R, Borgnakke C, Van Wylen G. Fundamentals of thermodynamics. The University of Michigan: Wiley; 1998.
29. Eisert J, Cramer M, Plenio MB. Area laws for the entanglement entropy. *Rev Mod Physics.* 2010;82(1):277–306.
30. Lambin P, Rios-Velazquez E, Leijenaar R, Carvalho S, van Stiphout RGPM, Granton P, et al. Radiomics: extracting more information from medical images using advanced feature analysis. *Eur J Cancer.* 2012;48(4):441–6.
31. Kumar V, Gu Y, Basu S, Berglund A, Eschrich SA, Schabath MB, et al. Radiomics: the process and the challenges. *Magn Reson Imaging.* 2012;30(9):1234–48.
32. Gillies RJ, Kinahan PE, Hricak H. Radiomics: Images Are More than Pictures, They Are Data. *Radiology.* 2015;278(2):563–77.
33. Raju VR, Anuradha B, Sreenivas B. Computational Intelligence in Subthalamic Nucleus Deep Brain Stimulation: Machine Learning Unsupervised PCA Tracking Method and Clustering Techniques for Parkinson's Feature Extraction. In: Gunjan, V.K., Suganthan, P.N., Haase, J., Kumar, (eds) *Cybernetics, Cognition and Machine Learning Applications. Algorithms for Intelligent Systems.* Springer, Singapore. 2023;37(9):1783–961.
34. Raju VR. Noise removal of deep brain stimulation artifacts in subthalamic nucleus neurons local field induced electrical potentials. *Indian J Neurosci.* 2022;8(2):130–7.
35. Raju VR, Reddy DA, Narsimha D, Srinivas K, Rani BK. Adaptive Closed-Loop Deep Brain Stimulator Coding Techniques for Target Detections in Parkinson's, Taylor & Francis Production (UK). *IETE J Res.* 2021:1-16.
36. Raju VR, Reddy A, Narsimha G. Deep Brain Stimulator Coding in Parkinson's: An Evolving Approach, Taylor & Francis Production (UK). *IETE J Res.* 2021:1-14.
37. Raju VR, Mridula RK, Borgohain R. Effect of Microelectrode Recording in Accurate Targeting STN with High Frequency DBS in Parkinson Disease, Taylor & Francis. *IETE J Res.* 2019;65(2):2019.
38. Raju VR. Principal component latent variate factorial analysis of MER signals of STN-DBS in Parkinson's disease (Electrode Implantation) Springer. *Nature.* 2018;68:3.
39. Raju VR, Rukmini KM, Borgohain R, P Ankathi Anitha SF Jabeen. "The Role of Microelectrode Recording (MER) in STN DBS Electrode Implantation", IFMBE Proceedings, Springer, Vol. 51, World Congress on Medical Physics and Biomedical Engineering, June 7-12, 2015, Toronto, Canada, Pp: 1204-1208, www.wc2015.org
40. Squire L, Berg D, Floyd E. Bloom, Sascha du Lac, Anirvan Ghosh Nicholas C. Spitzer, (2014) *Fundamental Neuroscience*, 4th Ed. AP Academic Press, 2014.
41. Raju VR, A Study of Advanced Multi-Channel EMG in Writer's Cramp, A PhD Thesis submitted to the Nizam's Institute of Medical Sciences (NIMS), Dec 2003, 2008.
42. Raju VR, Quantitative Multi-Channel EMG in Writer's Cramp, A MD/PhD Thesis submitted to the Nizam's Institute of Medical Sciences (NIMS), Dec 2003.

Cite this article. Raju VR. A study of artificial intelligence - Based machine learning and radiomic texture features in Parkinson's (Outcome of subthalamic nucleus deep brain stimulations analysis). *IP Indian J Neurosci* 2025;11(2):94-104.